

Mitigating Perception Bias: A Training-Free Approach to Enhance LMM for Image Quality Assessment

Siyi Pan¹ Baoliang Chen¹ Danni Huang¹ Hanwei Zhu²
Lingyu Zhu² Xiangjie Sui³ Shiqi Wang²

¹ South China Normal University ² City University of Hong Kong
³ City University of Macau

<https://barrypan12138.github.io/Q-Debias/>

Abstract

Despite the impressive performance of large multimodal models (LMMs) in high-level visual tasks, their capacity for image quality assessment (IQA) remains limited. One main reason is that LMMs are primarily trained for high-level tasks (e.g., image captioning), emphasizing unified image semantics extraction under varied quality. Such semantic-aware yet quality-insensitive perception bias inevitably leads to a heavy reliance on image semantics when those LMMs are forced for quality rating. In this paper, instead of retraining or tuning an LMM costly, we propose a training-free debiasing framework, in which the image quality prediction is rectified by mitigating the bias caused by image semantics. Specifically, we first explore several semantic-preserving distortions that can significantly degrade image quality while maintaining identifiable semantics. By applying these specific distortions to the query/test images, we ensure that the degraded images are recognized as poor quality while their semantics remain. During quality inference, both a query image and its corresponding degraded version are fed to the LMM along with a prompt indicating that the query image quality should be inferred under the condition that the degraded one is deemed poor quality. This prior condition effectively aligns the LMM’s quality perception, as all degraded images are consistently rated as poor quality, regardless of their semantic difference. Finally, the quality scores of the query image inferred under different prior conditions (degraded versions) are aggregated using a conditional probability model. Extensive experiments on various IQA datasets show that our debiasing framework could consistently enhance the LMM performance and the code will be publicly available.

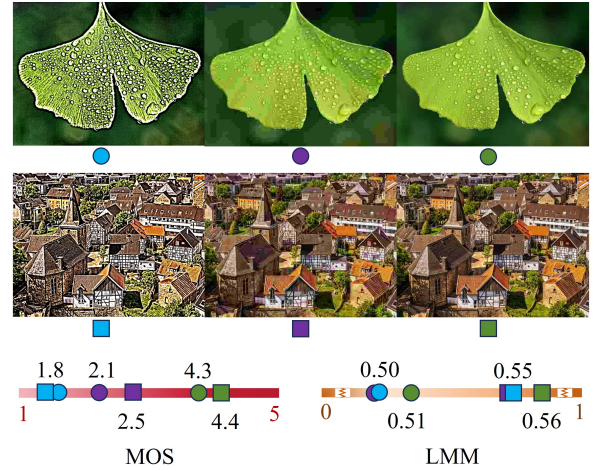


Figure 1. Illustration of perception bias in Large Multimodal Model (LMM) during quality assessment. Image quality ratings from the LMM (mPLUG-Owl3 [56]) were obtained using the Q-Bench testing framework [49]. The LMM consistently assigns higher quality ratings to images in the second row compared to the first, despite both sets exhibiting similar quality distributions as measured by Mean Opinion Scores (MOSs). This discrepancy suggests that the LMM relies more on image semantics than on low-level image clues for quality assessment. Zoom in for enhanced clarity.

1. Introduction

Image Quality Assessment (IQA) models aim to measure image quality in alignment with human perception, playing a fundamental role across various computer vision tasks [48]. According to the availability of reference information, the IQA models can be classified into Full-Reference IQA (FR-IQA), Reduced-Reference IQA (RR-IQA), and No-Reference IQA (NR-IQA) [60]. Among these, NR-IQA presents particular values as the image quality can be predicted without a reference requirement. In the past decades,

significant progress has been witnessed in NR-IQA, including traditional hand-crafted feature-based models [16, 31, 32, 34] and deep learning-based models [13, 20, 42, 64, 66]. Despite the advancement, current models still grapple with limited generalization capabilities on unseen scenes and distortions due to the significant distribution shifts between training and test sets. Recently, the emergence of Large Multimodal Models (LMMs) [37] has demonstrated impressive generalization abilities across various vision-language tasks, such as classification [47], image captioning [59], and visual question answering [40]. However, the focus on high-level visual tasks usually limits their effectiveness in low-level tasks, such as IQA [43, 49]. Although pioneering researchers have attempted to fine-tune or retrain LMMs for improved IQA accuracy [8, 50, 67], the laborious dataset construction and costly model training usually render this approach inefficient. Moreover, tuning LMMs specifically for IQA also introduces the risk of catastrophic forgetting [30], compromising the retention of general knowledge and ultimately degrading the models’ capability on other tasks.

A powerful strategy to both retain the LMM’s strengths across tasks and enhance its IQA performance is to unlock its vast general knowledge through well-crafted prompts, encouraging the LMM to respond accurately to quality rating requests. However, despite this potential, LMMs—driven by training objectives that emphasize semantic extraction over quality—usually default to *interpreting image quality heavily relying on image semantics*. As shown in Fig. 1, two sets of distorted images with different semantics are presented to an LMM for quality rating. The results indicate that the LMM consistently prefers the quality of images with the second set of semantics, despite both sets having similar quality (Mean Opinion Score (MOS)) distributions. The case reveals that the LMM intrinsically bases its quality rating on image semantics rather than on quality-related clues (*e.g.*, noise or blur).

Motivated by this observation, we introduce an innovative, training-free approach to mitigate the perception bias inherent in LMMs. Our enhancement strategy consists of two main steps: 1) *bias exposure*, and 2) *bias mitigation*. In the bias exposure step, we assume that the same bias exists consistently across images sharing the same semantics. Based on this assumption, we can expose the perception bias of a query/test image by measuring *how much the LMM resists labeling it as high quality when its quality is severely degraded but the semantics are preserved*. To achieve this, we explore several specific distortions that drastically corrupt the image quality while preserving its semantics to some extent. For a query image, we then impose these distortions on the query image and obtain its degraded versions. Herein, those degraded images should be deemed as poor quality. However, the LMM may not always agree

with the fact and the disagreement leads to the bias exposure. In the bias mitigation step, we address the exposed bias using an instructive conditional prompt. Specifically, during inference, we provide both the query image and its degraded version to the LMM, along with a prompt indicating that *the quality of the query image should be assessed under the condition that the degraded counterpart is rated as poor quality*. By forcing the LMM to rate the quality of the degraded images appropriately, the bias mitigation in turn refines the LMM’s quality prediction for the query image. Finally, the quality predictions under different distortions are aggregated through a conditional probability model, further improving the prediction accuracy. Before delving into detail, we highlight our main contributions as follows:

- **Investigation of Perception Bias in LMM for IQA.** We explore the perception bias inherent in LMM when used for IQA. Our training-free approach, which requires no task-specific fine-tuning, highlights a new pathway for leveraging pre-trained LMM on unseen tasks.
- **Conditional Prompt for Bias Mitigation.** We introduce a simple yet effective conditional prompt to mitigate the semantic bias in quality assessment. The prompt encourages the LMM to rate the image quality by aligning the quality prediction of synthetically degraded images, effectively reducing the bias caused by the semantics varies. Additionally, a confidence-based quality aggregation model is designed, further enhancing the prediction accuracy.
- **Comprehensive Evaluation on Diverse Datasets and Distortions.** We extensively evaluated our method on both natural and AI-generated images and the superior performance underscores the high effectiveness of our bias mitigation strategy. In addition, consistent improvements across multiple LMMs also demonstrate the strong generalization of our method, highlighting its potential to successfully extend to future LMMs.

2. Related work

NR-IQA. Traditional NR-IQA methods mainly rely on handcrafted features to model natural scene statistics (NSS) and estimate image quality by assessing the destruction level of the NSS. For example, Mean-Subtracted Contrast-Normalized (MSCN) coefficients were explored to model NSS as a unified distribution, enabling quality estimation through distributional discrepancy analysis [34]. Such NSS descriptors were also widely investigated in the wavelet domain [35, 44], gradient domain [54] as well as the discrete cosine transform (DCT) domain [39]. Drawing inspiration from the free-energy brain theory that the human visual system (HVS) strives to minimize uncertainty through an internal generative model [11, 12], psychovisual quality models were proposed in [16, 17, 61]. Tough valu-

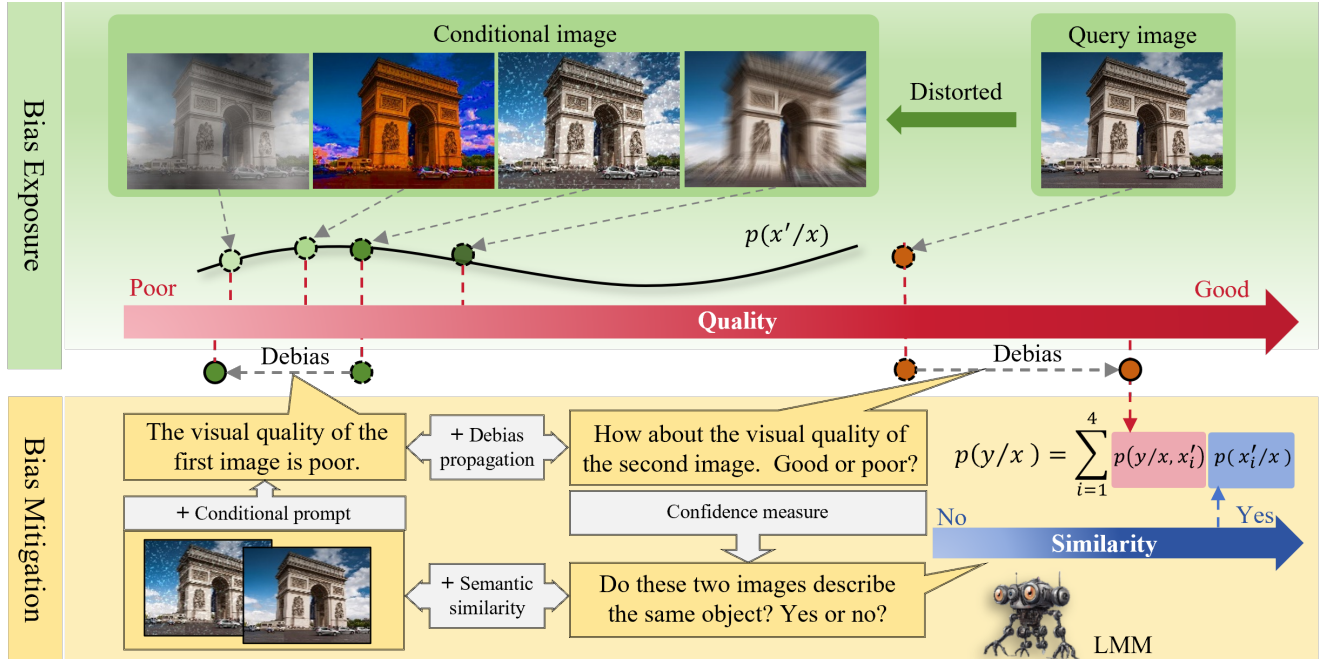


Figure 2. The framework of our perception bias mitigation scheme. It mainly consists of two components: 1) Bias Exposure: Specific distortions are imposed on the query image to significantly degrade the query image quality while preserving its semantics. The disagreement that the LMM rates those distorted images as poor quality exposes the perception bias inherent in the LMM. 2) Bias Mitigation: Dedicated prompts are defined to mitigate the bias by forcing that the quality of the query image should be assessed under the condition that its degraded counterpart is rated as poor quality. The final quality is then estimated by a semantic similarity based aggregation.

able insights from these studies, the inherent complexity of HVS continues to challenge feature design, prompting a shift toward data-driven feature learning. Kang *et al.* proposed the first convolutional neural networks (CNNs) for IQA and extended this work into a multi-task learning framework [20, 21]. Inspired by the success, more advanced networks have emerged including DIQaM [4], RankIQA [28], FPR [7], and GraphIQA [41]. However, limited data scales and learning strategies still restrict their generalization across different distributions. To account for this, some works leverage general knowledge learned from other tasks for IQA, such as image classification [57], image restoration [25], and image-language correspondence [38, 45]. Other attempts have been dedicated to the new learning paradigms, including meta learning [66], continual learning [65], curriculum learning [46], and domain adaptation/generalization [5, 6]. Despite the impressive progress, enhancing generalization in NR-IQA remains a significant challenge.

LMM-based IQA. Recently, high-performance LMMs such as ChatGPT-4v [37], LLaVA [26, 27], and mPLUG-Owl3 [56] have exhibited strong zero-shot transfer capabilities across various vision tasks, suggesting their potential applicability in the IQA task. Early efforts, such

as Q-Bench [49] and DepictQA [58], established comprehensive benchmarks to evaluate LMMs in low-level visual perception. In [67], Zhu *et al.* examined the IQA performance of LMMs under the two-alternative forced choice (2AFC) prompting. Instead of score regression, Q-Align [50] enabled LMMs to rate images at text-defined rating levels, excelling in both quality and aesthetic assessment tasks. By utilizing pre-trained LMMs and extensive datasets, recent studies have continued to improve IQA outcomes [51, 52, 68]. Although fine-tuning LMMs for IQA yields strong performance, it also poses the risk of catastrophic forgetting [30] problems, leading to the degraded generalization capability on other tasks. In light of these limitations, training-free approaches offer a more promising alternative to fully harness the extensive knowledge in LMMs for IQA. However, this strategy remains relatively underexplored.

3. Methodology

3.1. Preliminary

Given a query image x , the typical prompt for the LMM in IQA is exemplified as follows:

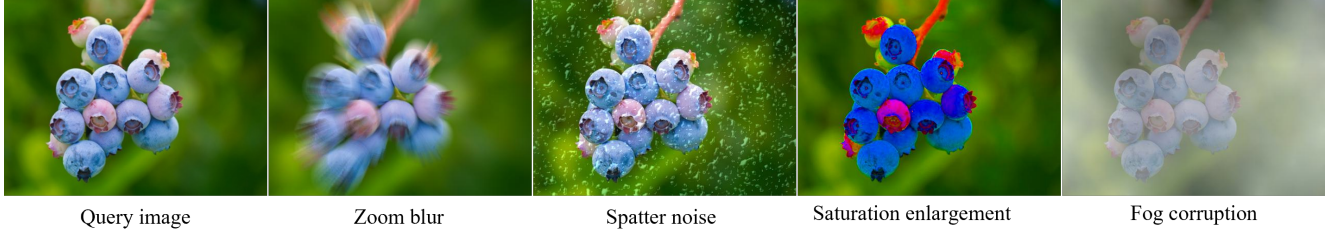


Figure 3. Illustration of the four distortion types which could degrade image quality significantly while largely preserving its semantics.

```
#User: Rate the quality of the image. Good
or poor? (Question) [IMAGE_TOKEN](Image)
#Assistant: The quality of the image is
[SCORE_TOKEN].
```

Based on the predicted logits of ‘good’ token (x^{gd}) and ‘poor’ token (x^{pr}) on the position of [SCORE_TOKEN], the image quality score y can be estimated by a SoftMax function:

$$p(y | x) = \frac{e^{x^{\text{gd}}}}{e^{x^{\text{gd}}} + e^{x^{\text{pr}}}}. \quad (1)$$

However, the semantic bias inherent in the LMM usually results in unreliable quality estimation, as the inference heavily relies on image semantics. To account for this, we adopt a conditional probability model to mitigate the bias, which can be formulated as follows,

$$p(y | x) = E_{x'|x} p(y | x, x') p(x' | x), \quad (2)$$

where x' is a “conditional image” of x , whose quality has been severely degraded while retaining similar semantics to x . $p(x' | x)$ represents the probability distribution of the potential degradation results. During inference, both the conditional image and the query image are fed to the LMM with a prompt instructing the LMM to rate the quality of the query image, under the condition that the conditional image is considered of poor quality. Our design philosophy is to guide the LMM toward confidently and accurately classifying the degraded images as poor quality, reducing its high reliance on image semantics in quality inference. This bias mitigation can, in turn, be propagated to the query image quality inference, assuming that the bias is consistently present in images with similar semantics but varying distortions.

3.2. Framework of Perception Bias Mitigation

Guided by the model constructed in Eqn. (2), we design our framework mainly comprises two components: 1) Bias Exposure. Specific distortions that significantly degrade image quality while preserving semantics are explored and imposed on the query image to construct different conditional images $p(x' | x)$. 2) Bias Mitigation. A dedicated

prompt is designed to estimate $p(y | x, x')$ across different conditional images and obtain the final quality by Eqn. (2). Our framework is illustrated in Fig. 2 and each component is detailed as follows.

3.2.1. Bias Exposure

Given a query image, we examine four typical distortions—zoom blur, spatter noise, saturation enlargement, and fog corruption—to effectively degrade the image quality while preserving its semantic content. Specifically:

Zoom Blur. The zoom blur distortion usually occurs when a camera moves toward an object rapidly, which can be simulated by

$$x'_1(u, v) = \frac{1}{n} \sum_{i=1}^n x_{z_i}(u, v), \quad (3)$$

where x_{z_i} means the zoom result of the query image x by a factor z_i and a total of n factors are adopted. $x'_0(u, v)$ means the zoom blur results at position (u, v) .

Spatter Noise. We use spatter noise to mimic the distortion caused by an unclean camera lens due to bad weather conditions such as rain, mud, or dust, which can be generated by

$$x'_2(u, v) = x(u, v) \cdot (1 - M(u, v)) + C(u, v) \cdot M(u, v), \quad (4)$$

where $M(u, v)$ is the spatter mask indicating regions that are affected or unaffected, and $C(u, v)$ represents the specific color distribution adapted for different splatter types. Herein, we use the implementation in [18] to generate $M(u, v)$ and $C(u, v)$.

Saturation Enlargement. The saturation distortion modifies the saturation channel of an image in the HSV color space based on the severity parameter c_0 , which can be defined by

$$x'_3 = f_{hsv2rgb}(x_h, x'_s, x_v), \quad (5)$$

with

$$x'_s = \text{clip}(x_s \cdot c, 0, 1), \quad (6)$$

where x_h, x_s , and x_v represent the hue, saturation, and value components of x in HSV space, respectively. x'_s denotes the distorted saturation. The function $f_{hsv2rgb}(\cdot)$ converts the image from HSV to RGB space, while $\text{clip}(\cdot)$ ensures that the distorted results are clipped to a valid range.

Fog Corruption. We simulate a foggy environment by applying a haze effect to the query image as follows:

$$x'_4 = \text{clip}(x + k \cdot x^F, 0, 1), \quad (7)$$

where the x^F is the fog pattern generated by a diamond-square algorithm [10, 18] based on x . k is the hyper-parameter of distortion severity. As shown in Fig. 3, the four types of distortion degrade the image quality significantly while the semantics are still recognizable, leading to an expected bias exposure when they are not deemed poor quality by the LMM.

3.2.2. Bias Mitigation

Based on the generated conditional images for each query image, we then input the query image (x) and one of its counterparts (x'_i) into the LMM, using a specific prompt to propagate the bias mitigation effect from the conditional image to the query image.

#User: The visual quality of the first image is poor. How about the visual quality of the second image? Good or poor? (Question)
`[IMAGE_TOKEN1, IMAGE_TOKEN2].(Image1, Image2)`
#Assistant: The quality of the image is `[SCORE_TOKEN]`.

Then, the conditional quality probability can be estimated as follows:

$$p(y | x, x'_i) = \frac{e^{x^{\text{gd}}}}{e^{x^{\text{gd}}} + e^{x^{\text{br}}}}. \quad (8)$$

Finally, we aggregate the quality estimation across the four distortion types:

$$p(y | x) = \sum_{i=1}^4 p(y | x, x'_i) p(x'_i | x), \quad (9)$$

where $p(x'_i | x)$ is the probability that the distorted image is adopted as the condition. We leverage the semantic similarity between x and x' to estimate this probability, based on the assumption that the more semantic information maintained, the more confidently the image can be considered as a condition. We achieve the semantic similarity estimation by feeding another prompt to the LMM as follows,

#User: Do these two images describe the same object? Yes or no? (Question)
#Assistant: `[SCORE_TOKEN]`.

This yields

$$p(x'_i | x) = \frac{e^{w_i}}{\sum_{i=1}^4 e^{w_i}}, \quad (10)$$

with

$$w_i = \frac{e^{x_i^{\text{yes}}}}{e^{x_i^{\text{yes}}} + e^{x_i^{\text{no}}}}. \quad (11)$$

4. Experiments

4.1. Experimental Settings

Datasets. We evaluate our method on six publicly available datasets: LIVE Challenge [14], KonIQ-10k [19], AGIQA-3k [23], KADID-10k [24], SPAQ [9] and SIQAD [55]. The KonIQ-10k, SPAQ, and LIVE Challenge datasets are in-the-wild image collections, featuring authentic distortions. KonIQ-10k and SPAQ datasets each contain over 10,000 images and the SPAQ dataset is specifically designed to assess the quality of images captured by smartphones. The KADID-10k dataset comprises 10,125 images with various systematic distortions. The AGIQA-3k dataset includes 2,900 images focused on AI-generated image quality assessment. The SIQAD dataset is constructed for screen content image (SCI) quality assessment and a total of 980 distorted SCIs are involved.

Comparison Methods. We denote our method as ‘‘Q-Debias’’ and compare its performance against both training-free (opinion-unaware) and training-based methods across multiple datasets. The training-free methods include BLINDS-II [35], QAC [53], BRISQUE [33], NIQE [34], ILNIQE [62], NPQI [29], ContentSep [2], CLIP-IQA [45], MDFS [36], and Q-Bench [49]. In particular, Q-Bench refers to using the same LMM (mPLUG-Owl3) with our method, while applying the query prompt from Q-Bench. For the training-based methods, we adopt models trained on the large-scale KonIQ-10k dataset for comparison, including ARNIQA [1], TReS [15], and MUSIQ [22]. We list their performance in cross-dataset settings to verify their generalization capability. The Pearson Linear Correlation Coefficient (PLCC) and the Spearman Rank-Order Correlation Coefficient (SRCC) are used as metrics to assess the linearity and monotonicity of our quality predictions.

Implementation Details. We select mPLUG-Owl3 as our LMM due to its superior performance on image processing tasks. We set $z_i \in \{1.00, 1.01, 1.02, \dots, 1.10\}$, $n = 11$ in Eqn. (3), and $c = 2.0$ in Eqn. (6). We set $k = 2.5$ in Eqn. (7). Our code is implemented in PyTorch and runs on an A6000 GPU.

4.2. Comparison with NR-IQA Models

Prediction Accuracy. As shown in Table 1, compared with existing training-free methods, our model Q-Debias

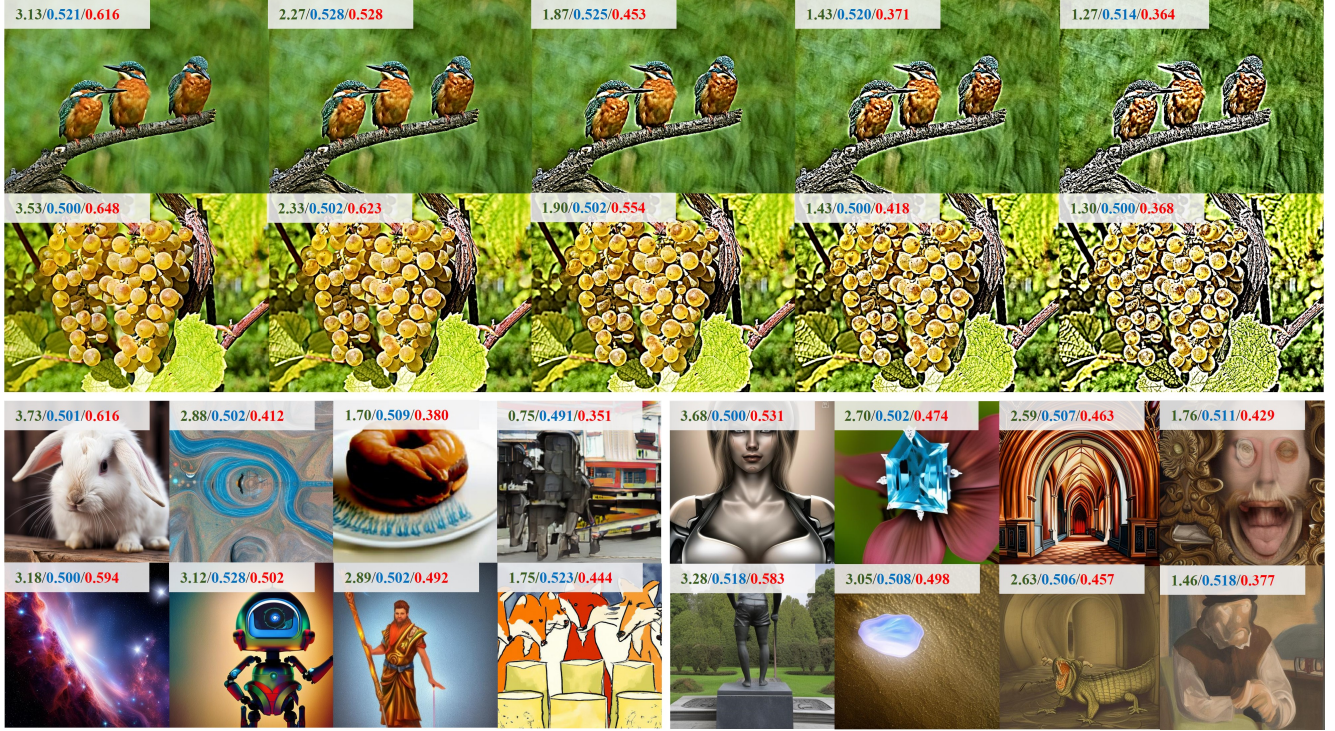


Figure 4. Visualization of image quality prediction results. In each subfigure, the top-left label shows numbers in green, blue, and red, representing the MOS, the LMM prediction result with the prompt in Q-Bench, and Our result, respectively.

Table 1. Performance comparison of our method, Q-Debias, against both training-free and training-based IQA models. The Red percentage indicates the improvement of our method over Q-Bench. ‘Sp’ indicates results predicted when only the spatter-noise-degraded image is utilized as a condition under our enhancement framework. The best two results are highlighted in boldface.

Methods	Training-free? (Training Set)	LIVE Challenge		KonIQ-10k		AGIQA-3k		KADID-10k		SPAQ		SIQAD	
		SRCC ↑	PLCC ↑	SRCC ↑	PLCC ↑	SRCC ↑	PLCC ↑	SRCC ↑	PLCC ↑	SRCC ↑	PLCC ↑	SRCC ↑	PLCC ↑
BLINDS-II [35]	✓	0.090	0.107	0.585	0.598	0.454	0.510	0.224	0.313	0.317	0.326	0.681	0.726
QAC [53]	✓	0.226	0.284	0.340	0.291	-	-	0.239	0.309	0.440	0.450	0.300	0.375
BRISQUE [33]	✓	0.561	0.598	0.705	0.707	0.493	0.533	0.330	0.370	0.484	0.481	0.157	0.215
NIQE [34]	✓	0.463	0.491	0.551	0.488	0.528	0.520	0.379	0.389	0.703	0.671	0.369	0.341
ILNIQE [62]	✓	0.439	0.503	0.505	0.496	0.594	0.623	0.540	0.534	0.696	0.637	0.375	0.385
NPQI [29]	✓	0.475	0.490	0.613	0.614	0.658	0.714	0.391	0.340	0.600	0.616	-	-
ContentSep [2]	✓	0.506	0.513	0.640	0.627	-	-	0.506	0.357	0.708	0.665	-	-
CLIP-IQA [45]	✓	0.612	0.594	0.695	0.727	0.658	0.714	0.500	0.520	0.738	0.735	0.596	0.657
MDFS [36]	✓	0.482	0.536	0.733	0.712	0.672	0.676	0.598	0.594	0.741	0.718	-	-
ARNIQA [1]	✗ (KonIQ-10k)	0.670	0.715	-	-	0.621	0.694	0.725	0.717	0.576	0.577	0.558	0.591
TReS [15]	✗ (KonIQ-10k)	0.771	0.805	-	-	0.652	0.737	0.468	0.492	0.418	0.417	0.572	0.625
MUSIQ [22]	✗ (KonIQ-10k)	0.788	0.824	-	-	0.630	0.722	0.556	0.575	0.726	0.738	0.554	0.598
Q-Bench* [49]	✓	0.721	0.677	0.672	0.573	0.596	0.469	0.315	0.267	0.767	0.650	0.333	0.402
Q-Debias (Ours)	✓	0.794	0.790	0.838	0.863	0.717	0.753	0.700	0.713	0.867	0.826	0.324	0.341
Improvement over Q-bench		↑10.1%	↑16.7%	↑24.7%	↑50.6%	↑20.3%	↑60.6%	↑122.2%	↑167.0%	↑13.0%	↑27.1%	Sp: 0.385 ↑18.8%	Sp: 0.427 ↑25.2%

* We use the same quality query prompt from Q-Bench and set the LMM as mPLUG-Owl3, consistent with our method.

consistently achieves the best performance across the first five IQA datasets. In particular, most hand-crafted feature-based models (e.g., NIQE) experience a significant performance drop on the KADID-10k dataset due to the diverse distortion types involved. However, our method still outperforms these models by a large margin, demonstrating its high effectiveness. Compared to the vanilla prompt used in Q-Bench, our method—while utilizing the same base LMM (mPLUG-Owl3)—achieves performance gains across all five datasets. Notably, both Q-Bench and our

method do not achieve promising results on the SIQAD dataset. The reason may lie in that LMMs are primarily trained on natural images, while the SCIs in the SIQAD dataset have been less extensively explored. From our experiments, we observe that not all distortion types for conditional image generation are effective for SIQAD. However, the introduction of single spatter noise demonstrates a positive effect on the SIQAD dataset, suggesting that our conditional prompt strategy can still be effective when specific distortions are carefully explored.

Table 2. Performance improvement on other LMMs.

Models	LIVE Challenge				AGIQA-3k				Average			
	Vanilla prompt		Our debias scheme		Vanilla prompt		Our debias scheme		Vanilla prompt		Our debias scheme	
	SRCC↑	PLCC↑	SRCC↑	PLCC↑	SRCC↑	PLCC↑	SRCC↑	PLCC↑	SRCC	PLCC	SRCC	PLCC
BakLLaVA [26]	0.090	0.108	0.263 (↑192.0%)	0.265 (↑145.0%)	0.480	0.321	0.460	0.482 (↑50.2%)	0.285	0.215	0.362 (↑27.0%)	0.374 (↑74.0%)
Qwen-VL [3]	0.470	0.546	0.504 (↑7.20%)	0.501	0.504	0.532	0.615 (↑22.0%)	0.623 (↑17.1%)	0.487	0.539	0.560 (↑15.0%)	0.562 (↑4.27%)

Table 3. Ablation study of different types of conditional images. The best two results are highlighted in boldface.

Exp. ID	Setting					LIVE Challenge		SIQAD		AGIQA-3k	
	Zoom	Spatter	Fog	Saturation	Semantic consistency	SRCC↑	PLCC↑	SRCC↑	PLCC↑	SRCC↑	PLCC↑
1	✗	✗	✗	✗	✗	0.721	0.677	0.333	0.402	0.596	0.469
2	✓	✗	✗	✗	✓	0.644	0.489	0.197	0.168	0.633	0.539
3	✗	✓	✗	✗	✓	0.762	0.694	0.385	0.427	0.713	0.704
4	✗	✗	✓	✗	✓	0.726	0.615	0.354	0.325	0.685	0.644
5	✗	✗	✗	✓	✓	0.784	0.790	0.265	0.258	0.720	0.735
6	✗	✓	✗	✓	✓	0.793	0.790	0.335	0.294	0.709	0.712
7	✗	✓	✓	✓	✓	0.793	0.773	0.349	0.308	0.714	0.702
8	✓	✓	✓	✓	✗	0.714	0.620	0.114	0.128	0.707	0.613
Q-Debias	✓	✓	✓	✓	✓	0.794	0.790	0.326	0.341	0.717	0.753

In comparison to training-free methods, training-based models generally deliver superior results, benefiting from the quality assessment knowledge learned from large-scale datasets. However, due to the fact that KonIQ-10k only contains authentic distortions, these models often underperform on unseen distortions when tested on datasets involving unseen distortions (e.g., TReS: 0.771 on LIVE Challenge vs 0.468 on KADID-10k, MUSIQ: 0.788 on LIVE Challenge vs 0.630 on AGIQA-3k), highlighting the overfitting dilemma during training. In contrast, our approach improves the LMM in a training-free manner, providing superior generalization capability across authentic, systemic, and AI-generated distortions.

Visualization. To verify the effectiveness of our method, we visualize our predicted results alongside the LMM predictions using the Q-Bench prompt on the KADID-10k dataset (first two rows) and the AIGC-3k dataset (second two rows). As shown in Fig. 4, we can observe that: 1) Despite comparable distortions and closely aligned MOS distributions in the first two rows, the LMM without our debiasing enhancement consistently assigns higher quality ratings to images in the first row over the second. This observation underscores the model’s high reliance on semantic content rather than low-level clues for quality assessment, revealing the presence of perceptual bias. 2) The bias varies by semantic content, affecting both natural and AI-generated images. In contrast, our debias strategy could effectively mitigate such bias, resulting in predictions that are more consistent with human ratings (*i.e.*, MOSs).

4.3. Generalization on Other LMMs

In our method, we adopted the multimodal model mPLUG-Owl3 as our foundation model. To demonstrate the generalization capability of our enhancement strategy, we further validate it on another two LMMs inducing: BakLLaVA [26], and Qwen-VL [3]. As shown in Table 2, we could observe a consistent average performance gains can be achieved. Notably, the improvements observed on the LIVE Challenge and AGIQA-3k datasets suggest that semantic bias is widespread across diverse content types and such bias can be mitigated by our method efficiently. The promising generalization capability highlights the transformative potential of our bias-mitigation strategy and opens up exciting new avenues for developing training-free enhancement methods to fully harness the potential of LMMs for unseen tasks.

Table 4. Study of instructive prompt.

Prompt	LIVE Challenge		KonIQ-10k		AGIQA-3k	
	SRCC↑	PLCC↑	SRCC↑	PLCC↑	SRCC↑	PLCC↑
T1	0.784	0.762	0.805	0.816	0.703	0.682
T2	0.785	0.762	0.813	0.847	0.705	0.702
T3	0.741	0.730	0.811	0.845	0.672	0.686
Q-Debias	0.794	0.790	0.838	0.863	0.717	0.753

4.4. Ablation Studies

Three main components are designed in our debias scheme: 1) the conditional images, 2) the instructive prompt, and 3) the aggregation scheme. To verify the effectiveness of each component, we ablate each component from our scheme and verify their effectiveness as follows.

Table 5. Study of different aggregation schemes.

Aggregation Scheme	LIVE Challenge		KonIQ-10k		AGIQA-3k	
	SRCC \uparrow	PLCC \uparrow	SRCC \uparrow	PLCC \uparrow	SRCC \uparrow	PLCC \uparrow
Average	0.789	0.754	0.824	0.838	0.711	0.691
Quality Similarity	0.785	0.740	0.817	0.827	0.710	0.683
Winner-Takes- All	0.632	0.491	0.750	0.660	0.623	0.529
Q-Debias	0.794	0.790	0.838	0.863	0.717	0.753

Study of Conditional Images. As shown in Table 3, we compare our method with eight types of variants: (1) no conditional images, (2)-(5) each variant with a single image, distorted by one of the four distortion types individually, (6) two images with the top two performing distortion types, (7) three images with the top three performing distortion types, and (8) the conditional images with semantics that do not match the query image. To establish a representative baseline, we first select images from open-source datasets that do not share semantics with those in the LIVE Challenge, SIQAD, and AGIQA-3k datasets. Four specific distortions are then applied to these selected images to create an additional conditional image set. Finally, we randomly select four low-quality images from this set as the conditional images. The results reveal that: 1) Each distortion type contributes positively to our final image quality prediction, with the Saturate distortion achieving the highest performance on the natural images and generated images (LIVE Challenge and AGIQA-3k datasets). 2) Combining multiple conditional images leads to final performance improvements, highlighting the complementary roles of the four distortion types. 3) A significant performance drop can be witnessed when semantically inconsistent images are used as conditions, underscoring the critical importance of semantic correspondence in bias mitigation. This reveals that bias is highly semantic-specific; using conditional images with matching semantics to the query image enables remarkably accurate bias estimation and consistently enhances quality prediction.

Study of Instructive Prompt. In our method, the prompt serves an instructive role for the LMM, facilitating the propagation of bias mitigation from the conditional images to the query image. To verify its effectiveness, we compare our method against three prompt variants: (T1) Prompt Replacement: The entire prompt is replaced with “Rate the quality of the second image. Good or poor?” (T2) Bias Exposure Ablation: The phrase “The visual quality of the first image is poor” is removed from our prompt to examine the role of bias exposure, leading to the second prompt: “How about the visual quality of the second image? Good or poor?”

(T3) Bias Mitigation Propagation Ablation: We delete the “How about” from the prompt to assess the impact of bias mitigation propagation to the query image, resulting in the third prompt: “The visual quality of the first image is poor. Rate the visual quality of the second image. Good or poor?” As shown in Table 4, the results reveal that: 1) Without our instructive prompt, even with the conditional images provided, bias cannot be effectively mitigated. 2) Without the explicit indication that the conditional images are of poor quality, the LMM fails to recognize the bias exposure, resulting in a marked performance drop. 3) The phrase “How about” suggests that the LMM should infer the query image’s quality based on the prior understanding that the conditional images are of poor quality. Without this phrase, the propagation of bias mitigation from the conditional images to the query image weakens noticeably. The best results are achieved when the full prompt is included, demonstrating the necessity of each instruction in our prompt.

Study of Aggregation Scheme. To aggregate the quality scores derived from different conditional images, we introduce a semantic similarity aggregation strategy. To assess its effectiveness, we compare our method with four alternative schemes: 1) Average Aggregation: Each of the four quality scores is assigned an equal weight during aggregation. 2) Quality Similarity Aggregation: We utilize the widely adopted FR-IQA model, LPIPS [63], to measure the quality similarity between the query image and each of its conditional images. These quality similarity scores are then treated as weights for the aggregation. 3) Winner-Takes-All: The final quality score is determined solely by the quality score obtained from the conditional image that exhibits the highest semantic similarity to the query image. The results are presented in Table 5, which reveal that: 1) The Average scheme results in a noticeable performance drop, suggesting that uniform weighting fails to account for the bias variations across different types of distortions. 2) The Quality Similarity scheme is also ineffective. The possible reason may lie that a higher quality similarity score does not always correspond to a higher semantic recognition for the LMM, due to perceptual discrepancy between the LMM and the human visual system. 3) The Winner-Takes-All scheme, though commonly used for score aggregation, demonstrates suboptimal performance as it fails to adequately capture the nuanced contributions of different conditional images. In comparison, our semantic similarity aggregation scheme delivers the best performance across datasets containing synthetic, authentic, and generative distortions, demonstrating its superior generalization on diverse image distortions.

5. Conclusion

In this paper, we propose a training-free scheme to enhance the LMM in the IQA task. In particular, the perception bias that the LMM infers image quality highly relies on image semantics is mitigated by introducing conditional images in the prompt. These conditional images share the similar semantics as the query image but experience degraded quality. By instructing the LMM to align its quality ratings on those conditional images, the alignment in turn forces the LMM to rectify their judgment on the query image. Experimental results on images with different distortions verify the effectiveness of our method, and the generalization capability of our scheme across other LMMs highlights the potential for advanced prompt designs to fully leverage LMM knowledge for unseen tasks.

References

- [1] Lorenzo Agnolucci, Leonardo Galteri, Marco Bertini, and Alberto Del Bimbo. Arniqa: Learning distortion manifold for image quality assessment. In *IEEE Winter Conference on Applications of Computer Vision*, pages 189–198, 2024. 5, 6
- [2] Nithin C Babu, Vignesh Kannan, and Rajiv Soundararajan. No reference opinion unaware quality assessment of authentically distorted images. In *IEEE Winter Conference on Applications of Computer Vision*, pages 2459–2468, 2023. 5, 6
- [3] Jinze Bai, Shuai Bai, Shusheng Yang, Shijie Wang, Sinan Tan, Peng Wang, Junyang Lin, Chang Zhou, and Jingren Zhou. Qwen-vl: A frontier large vision-language model with versatile abilities. *arXiv preprint arXiv:2308.12966*, 2023. 7
- [4] Sebastian Bosse, Dominique Maniry, Klaus-Robert Müller, Thomas Wiegand, and Wojciech Samek. Deep neural networks for no-reference and full-reference image quality assessment. *IEEE Transactions on Image Processing*, 27(1):206–219, 2017. 3
- [5] Baoliang Chen, Haoliang Li, Hongfei Fan, and Shiqi Wang. No-reference screen content image quality assessment with unsupervised domain adaptation. *IEEE Transactions on Image Processing*, 30:5463–5476, 2021. 3
- [6] Baoliang Chen, Lingyu Zhu, Guo Li, Fangbo Lu, Hongfei Fan, and Shiqi Wang. Learning generalized spatial-temporal deep feature representation for no-reference video quality assessment. *IEEE Transactions on Circuits and Systems for Video Technology*, 32(4):1903–1916, 2021. 3
- [7] Baoliang Chen, Lingyu Zhu, Chenqi Kong, Hanwei Zhu, Shiqi Wang, and Zhu Li. No-reference image quality assessment by hallucinating pristine features. *IEEE Transactions on Image Processing*, 31:6139–6151, 2022. 3
- [8] Chaofeng Chen, Sensen Yang, Haoning Wu, Liang Liao, Zicheng Zhang, Annan Wang, Wenxiu Sun, Qiong Yan, and Weisi Lin. Q-Ground: Image quality grounding with large multi-modality models. In *ACM International Conference on Multimedia*, pages 486–495, 2024. 2
- [9] Yuming Fang, Hanwei Zhu, Yan Zeng, Kede Ma, and Zhou Wang. Perceptual quality assessment of smartphone photography. In *IEEE Conference on Computer Vision and Pattern Recognition*, pages 3677–3686, 2020. 5
- [10] Alain Fournier, Don Fussell, and Loren Carpenter. Computer rendering of stochastic models. *Communications of the ACM*, 25(6):371–384, 1982. 5
- [11] Karl Friston. The free-energy principle: a unified brain theory? *Nature Reviews Neuroscience*, 11(2):127–138, 2010. 2
- [12] Karl Friston, James Kilner, and Lee Harrison. A free energy principle for the brain. *Journal of Physiology-Paris*, 100(1-3):70–87, 2006. 2
- [13] Yixuan Gao, Xiongkuo Min, Yucheng Zhu, Jing Li, Xiaoping Zhang, and Guangtao Zhai. Image quality assessment: From mean opinion score to opinion score distribution. In *ACM International Conference on Multimedia*, pages 997–1005, 2022. 2
- [14] Deepti Ghadiyaram and Alan C Bovik. Massive online crowdsourced study of subjective and objective picture quality. *IEEE Transactions on Image Processing*, 25(1):372–387, 2015. 5
- [15] S Alireza Golestaneh, Saba Dadsetan, and Kris M Kitani. No-reference image quality assessment via transformers, relative ranking, and self-consistency. In *IEEE Winter Conference on Applications of Computer Vision*, pages 3209–3218, 2022. 5, 6
- [16] Ke Gu, Guangtao Zhai, Xiaokang Yang, Wenjun Zhang, and Longfei Liang. No-reference image quality assessment metric by combining free energy theory and structural degradation model. In *IEEE International Conference on Multimedia and Expo (ICME)*, pages 1–6, 2013. 2
- [17] Ke Gu, Guangtao Zhai, Xiaokang Yang, and Wenjun Zhang. Using free energy principle for blind image quality assessment. *IEEE Transactions on Multimedia*, 17(1):50–63, 2014. 2
- [18] Dan Hendrycks and Thomas Dietterich. Benchmarking neural network robustness to common corruptions and perturbations. *International Conference on Learning Representations*, 2019. 4, 5
- [19] V. Hosu, H. Lin, T. Sziranyi, and D. Saupe. Koniq-10k: An ecologically valid database for deep learning of blind image quality assessment. *IEEE Transactions on Image Processing*, 29:4041–4056, 2020. 5
- [20] Le Kang, Peng Ye, Yi Li, and David Doermann. Convolutional neural networks for no-reference image quality assessment. In *IEEE Conference on Computer Vision and Pattern Recognition*, pages 1733–1740, 2014. 2, 3
- [21] Le Kang, Peng Ye, Yi Li, and David Doermann. Simultaneous estimation of image quality and distortion via multi-task convolutional neural networks. In *IEEE International Conference on Image Processing*, pages 2791–2795, 2015. 3
- [22] Junjie Ke, Qifei Wang, Yilin Wang, Peyman Milanfar, and Feng Yang. Musiq: Multi-scale image quality transformer. In *IEEE international conference on computer vision*, pages 5148–5157, 2021. 5, 6
- [23] Chunyi Li, Zicheng Zhang, Haoning Wu, Wei Sun, Xiongkuo Min, Xiaohong Liu, Guangtao Zhai, and Weisi

- Lin. AGIQA-3K: An open database for ai-generated image quality assessment. *IEEE Transactions on Circuits and Systems for Video Technology*, pages 1–1, 2023. 5
- [24] Hanhe Lin, Vlad Hosu, and Dietmar Saupe. Kadid-10k: A large-scale artificially distorted iqa database. In *International Conference on Quality of Multimedia Experience*, pages 1–3, 2019. 5
- [25] Kwan-Yee Lin and Guanxiang Wang. Hallucinated-IQA: No-reference image quality assessment via adversarial learning. In *IEEE Conference on Computer Vision and Pattern Recognition*, pages 732–741, 2018. 3
- [26] Haotian Liu, Chunyuan Li, Yuheng Li, and Yong Jae Lee. Improved baselines with visual instruction tuning. In *IEEE Conference on Computer Vision and Pattern Recognition*, pages 26296–26306, 2024. 3, 7
- [27] Haotian Liu, Chunyuan Li, Qingyang Wu, and Yong Jae Lee. Visual instruction tuning. *Advances in neural information processing systems*, 36, 2024. 3
- [28] Xialei Liu, Joost van de Weijer, and Andrew D Bagdanov. RankIQA: Learning from rankings for no-reference image quality assessment. In *IEEE International Conference on Computer Vision*, pages 1040–1049, 2017. 3
- [29] Yutao Liu, Ke Gu, Xiu Li, and Yongbing Zhang. Blind image quality assessment by natural scene statistics and perceptual characteristics. *ACM Transactions on Multimedia Computing, Communications, and Applications*, 16(3):1–91, 2020. 5, 6
- [30] Yun Luo, Zhen Yang, Fandong Meng, Yafu Li, Jie Zhou, and Yue Zhang. An empirical study of catastrophic forgetting in large language models during continual fine-tuning. *arXiv preprint arXiv:2308.08747*, 2023. 2, 3
- [31] Xiongkuo Min, Ke Gu, Guangtao Zhai, Jing Liu, Xiaokang Yang, and Chang Wen Chen. Blind quality assessment based on pseudo-reference image. *IEEE Transactions on Multimedia*, 20(8):2049–2062, 2017. 2
- [32] Xiongkuo Min, Kede Ma, Ke Gu, Guangtao Zhai, Zhou Wang, and Weisi Lin. Unified blind quality assessment of compressed natural, graphic, and screen content images. *IEEE Transactions on Image Processing*, 26(11):5462–5474, 2017. 2
- [33] Anish Mittal, Anush Krishna Moorthy, and Alan Conrad Bovik. No-reference image quality assessment in the spatial domain. *IEEE Transactions on Image Processing*, 21(12):4695–4708, 2012. 5, 6
- [34] Anish Mittal, Rajiv Soundararajan, and Alan C Bovik. Making a “completely blind” image quality analyzer. *IEEE Signal Processing Letters*, 20(3):209–212, 2012. 2, 5, 6
- [35] Anush Krishna Moorthy and Alan Conrad Bovik. A two-step framework for constructing blind image quality indices. *IEEE Signal Processing Letters*, 17(5):513–516, 2010. 2, 5, 6
- [36] Zhangkai Ni, Yue Liu, Keyan Ding, Wenhan Yang, Hanli Wang, and Shiqi Wang. Opinion-unaware blind image quality assessment using multi-scale deep feature statistics. *IEEE Transactions on Multimedia*, 2024. 5, 6
- [37] OpenAI. OpenAI. GPT-4V(ision) system card. Technical report, OpenAI, 2023. 2, 3
- [38] Alec Radford, Jong Wook Kim, Chris Hallacy, Aditya Ramesh, Gabriel Goh, Sandhini Agarwal, Girish Sastry, Amanda Askell, Pamela Mishkin, Jack Clark, et al. Learning transferable visual models from natural language supervision. In *International conference on machine learning*, pages 8748–8763. PMLR, 2021. 3
- [39] Michele A Saad, Alan C Bovik, and Christophe Charrier. Blind image quality assessment: A natural scene statistics approach in the dct domain. *IEEE Transactions on Image Processing*, 21(8):3339–3352, 2012. 2
- [40] Chuyi Shang, Amos You, Sanjay Subramanian, Trevor Darrell, and Roei Herzig. Traveler: A modular multi-lmm agent framework for video question-answering. *arXiv preprint arXiv:2404.01476*, 2024. 2
- [41] Simen Sun, Tao Yu, Jiahua Xu, Wei Zhou, and Zhibo Chen. GraphIQA: Learning distortion graph representations for blind image quality assessment. *IEEE Transactions on Multimedia*, 2022. 3
- [42] Wei Sun, Xiongkuo Min, Danyang Tu, Siwei Ma, and Guangtao Zhai. Blind quality assessment for in-the-wild images via hierarchical feature fusion and iterative mixed database training. *IEEE Journal of Selected Topics in Signal Processing*, 17(6):1178–1192, 2023. 2
- [43] Yinan Sun, Zicheng Zhang, Haoning Wu, Xiaohong Liu, Weisi Lin, Guangtao Zhai, and Xiongkuo Min. Explore the hallucination on low-level perception for mllms. *arXiv preprint arXiv:2409.09748*, 2024. 2
- [44] Huixuan Tang, Neel Joshi, and Ashish Kapoor. Learning a blind measure of perceptual image quality. In *IEEE Conference on Computer Vision and Pattern Recognition*, pages 305–312, 2011. 2
- [45] Jianyi Wang, Kelvin CK Chan, and Chen Change Loy. Exploring clip for assessing the look and feel of images. In *Proceedings of the AAAI Conference on Artificial Intelligence*, pages 2555–2563, 2023. 3, 5, 6
- [46] Juan Wang, Zewen Chen, Chunfeng Yuan, Bing Li, Wentao Ma, and Weiming Hu. Hierarchical curriculum learning for no-reference image quality assessment. *International Journal of Computer Vision*, 131(11):3074–3093, 2023. 3
- [47] Xiao Wang, Guangyao Chen, Guangwu Qian, Pengcheng Gao, Xiao-Yong Wei, Yaowei Wang, Yonghong Tian, and Wen Gao. Large-scale multi-modal pre-trained models: A comprehensive survey. *Machine Intelligence Research*, 20(4):447–482, 2023. 2
- [48] Zhou Wang and Alan Conrad Bovik. *Modern image quality assessment*. PhD thesis, Springer, 2006. 1
- [49] Haoning Wu, Zicheng Zhang, Erli Zhang, Chaofeng Chen, Liang Liao, Annan Wang, Chunyi Li, Wenxiu Sun, Qiong Yan, Guangtao Zhai, et al. Q-bench: A benchmark for general-purpose foundation models on low-level vision. *arXiv preprint arXiv:2309.14181*, 2023. 1, 2, 3, 5, 6
- [50] Haoning Wu, Zicheng Zhang, Weixia Zhang, Chaofeng Chen, Liang Liao, Chunyi Li, Yixuan Gao, Annan Wang, Erli Zhang, Wenxiu Sun, et al. Q-align: Teaching llms for visual scoring via discrete text-defined levels. *arXiv preprint arXiv:2312.17090*, 2023. 2, 3
- [51] Haoning Wu, Zicheng Zhang, Erli Zhang, Chaofeng Chen, Liang Liao, Annan Wang, Kaixin Xu, Chunyi Li, Jingwen

- Hou, Guangtao Zhai, et al. Q-instruct: Improving low-level visual abilities for multi-modality foundation models. In *IEEE Conference on Computer Vision and Pattern Recognition*, pages 25490–25500, 2024. 3
- [52] Haoning Wu, Hanwei Zhu, Zicheng Zhang, Erli Zhang, Chaofeng Chen, Liang Liao, Chunyi Li, Annan Wang, Wenxiu Sun, Qiong Yan, et al. Towards open-ended visual quality comparison. *arXiv preprint arXiv:2402.16641*, 2024. 3
- [53] Wufeng Xue, Lei Zhang, and Xuanqin Mou. Learning without human scores for blind image quality assessment. In *IEEE Conference on Computer Vision and Pattern Recognition*, pages 995–1002, 2013. 5, 6
- [54] Wufeng Xue, Xuanqin Mou, Lei Zhang, Alan C Bovik, and Xiangchu Feng. Blind image quality assessment using joint statistics of gradient magnitude and laplacian features. *IEEE Transactions on Image Processing*, 23(11):4850–4862, 2014. 2
- [55] Huan Yang, Yuming Fang, and Weisi Lin. Perceptual quality assessment of screen content images. *IEEE Transactions on Image Processing*, 24(11):4408–4421, 2015. 5
- [56] Jiabo Ye, Haiyang Xu, Haowei Liu, Anwen Hu, Ming Yan, Qi Qian, Ji Zhang, Fei Huang, and Jingren Zhou. mplug-owl3: Towards long image-sequence understanding in multi-modal large language models. *arXiv preprint arXiv:2408.04840*, 2024. 1, 3
- [57] Junyong You and Jari Korhonen. Transformer for image quality assessment. In *IEEE International Conference on Image Processing (ICIP)*, pages 1389–1393. IEEE, 2021. 3
- [58] Zhiyuan You, Jinjin Gu, Zheyuan Li, Xin Cai, Kaiwen Zhu, Tianfan Xue, and Chao Dong. Descriptive image quality assessment in the wild. *arXiv preprint arXiv:2405.18842*, 2024. 3
- [59] Weihao Yu, Zhengyuan Yang, Linjie Li, Jianfeng Wang, Kevin Lin, Zicheng Liu, Xinchao Wang, and Lijuan Wang. Mm-vet: Evaluating large multimodal models for integrated capabilities. *arXiv preprint arXiv:2308.02490*, 2023. 2
- [60] Guangtao Zhai and Xiongkuo Min. Perceptual image quality assessment: a survey. *Science China Information Sciences*, 63:1–52, 2020. 1
- [61] Guangtao Zhai, Xiaolin Wu, Xiaokang Yang, Weisi Lin, and Wenjun Zhang. A psychovisual quality metric in free-energy principle. *IEEE Transactions on Image Processing*, 21(1): 41–52, 2011. 2
- [62] Lin Zhang, Lei Zhang, and Alan C Bovik. A feature-enriched completely blind image quality evaluator. *IEEE Transactions on Image Processing*, 24(8):2579–2591, 2015. 5, 6
- [63] Richard Zhang, Phillip Isola, Alexei A Efros, Eli Shechtman, and Oliver Wang. The unreasonable effectiveness of deep features as a perceptual metric. In *IEEE Conference on Computer Vision and Pattern Recognition*, pages 586–595, 2018. 8
- [64] Weixia Zhang, Kede Ma, Jia Yan, Dexiang Deng, and Zhou Wang. Blind image quality assessment using a deep bilinear convolutional neural network. *IEEE Transactions on Circuits and Systems for Video Technology*, 30(1):36–47, 2018. 2
- [65] Weixia Zhang, Kede Ma, Guangtao Zhai, and Xiaokang Yang. Task-specific normalization for continual learning of blind image quality models. *IEEE Transactions on Image Processing*, 2024. 3
- [66] Hancheng Zhu, Leida Li, Jinjian Wu, Weisheng Dong, and Guangming Shi. MetaIQA: Deep meta-learning for no-reference image quality assessment. In *IEEE Conference on Computer Vision and Pattern Recognition (CVPR)*, pages 14143–14152, 2020. 2, 3
- [67] Hanwei Zhu, Xiangjie Sui, Baoliang Chen, Xuelin Liu, Peilin Chen, Yuming Fang, and Shiqi Wang. 2afc prompting of large multimodal models for image quality assessment. *arXiv preprint arXiv:2402.01162*, 2024. 2, 3
- [68] Hanwei Zhu, Haoning Wu, Yixuan Li, Zicheng Zhang, Baoliang Chen, Lingyu Zhu, Yuming Fang, Guangtao Zhai, Weisi Lin, and Shiqi Wang. Adaptive image quality assessment via teaching large multimodal model to compare. *arXiv preprint arXiv:2405.19298*, 2024. 3